Epithelial HIF-1α/claudin-1 axis regulates barrier dysfunction in eosinophilic esophagitis

Joanne C. Masterson,[1,2,3] Kathryn A. Biette,[2,3] Juliet A. Hammer,[2,3] Nathalie Nguyen,[2,3] Kelley E. Capocelli,[4] Bejan J. Saeedi,[3] Rachel F. Harris,[2,3] Shahan D. Fernando,[2,3] Lindsay B. Hosford,[2,3] Caleb J. Kelly,[3] Eric L. Campbell,[3] Stefan F. Ehrentraut,[3] Faria N. Ahmed,[2] Hiroshi Nakagawa,[5] James J. Lee,[6] Eóin N. McNamee,[1,3] Louise E. Glover,[3] Sean P. Colgan,[3] and Glenn T. Furuta[2,3]

[1]Allergy, Inflammation and Remodeling Research Laboratory, Human Health Research Institute, Department of Biology, Maynooth University, Maynooth, Co. Kildare, Ireland. [2]Gastrointestinal Eosinophilic Diseases Program, Department of Pediatrics, University of Colorado School of Medicine; Digestive Health Institute, Children's Hospital Colorado; Aurora, Colorado, USA. [3]Mucosal Inflammation Program, Department of Medicine, University of Colorado, Aurora, Colorado, USA. [4]Department of Pathology, Children's Hospital Colorado, Aurora, Colorado, USA. [5]Division of Gastroenterology, Department of Medicine, University of Pennsylvania Perelman School of Medicine, Philadelphia, Pennsylvania, USA. [6]Mayo Clinic, Scottsdale, Arizona, USA.

Epithelial barrier dysfunction is a significant factor in many allergic diseases, including eosinophilic esophagitis (EoE). Infiltrating leukocytes and tissue adaptations increase metabolic demands and decrease oxygen availability at barrier surfaces. Understanding of how these processes impact barrier is limited, particularly in allergy. Here, we identified a regulatory axis whereby the oxygen-sensing transcription factor *HIF-1α* orchestrated epithelial barrier integrity, selectively controlling tight junction *CLDN1* (claudin-1). Prolonged experimental hypoxia or *HIF1A* knockdown suppressed HIF-1α–dependent claudin-1 expression and epithelial barrier function, as documented in 3D organotypic epithelial cultures. L2-IL5^{OXA} mice with EoE-relevant allergic inflammation displayed localized eosinophil oxygen metabolism, tissue hypoxia, and impaired claudin-1 barrier via repression of HIF-1α/claudin-1 signaling, which was restored by transgenic expression of esophageal epithelial-targeted stabilized *HIF-1α*. EoE patient biopsy analysis identified a repressed HIF-1α/claudin-1 axis, which was restored via pharmacologic HIF-1α stabilization ex vivo. Collectively, these studies reveal HIF-1α's critical role in maintaining barrier and highlight the HIF-1α/claudin-1 axis as a potential therapeutic target for EoE.

Introduction

Intact epithelial-immune barriers play a critical role in maintaining a physical defense between external environmental antigens and the internal immune system. In allergy, epithelial barriers are often dysfunctional, contributing to pathophysiologic mechanisms of atopic diseases, including atopic dermatitis, asthma, and eosinophilic esophagitis (EoE). Patients with EoE are likely to have multiple comorbid atopy and are considered part of the so-called atopic march (1). It is widely understood that genetic elements, environmental factors, and abnormal inflammatory or developmental signaling pathways may all contribute to the establishment and maintenance of a defective epithelial barrier in allergy, leading to increased exposure to environmental or food antigens, allergic sensitization, and the development of chronic allergic inflammatory diseases.

Clinical experience and basic studies state that these principles are also true in EoE, a rapidly emerging disease. Genome-wide association studies have identified epithelial barrier–related genes such as *FLG* and *CAPN14* (2, 3). Transcriptomic studies have identified others associated with disease, including *SPINK7* and *SLC9A3* (4, 5). Histologic and ultrastructural studies revealed increased intercellular spaces and reduced desmosomal infrastructure (6–8), functional studies identified increased impedance (9), and molecular examinations determined key roles for inflammatory molecules including the cytokine IL-13 in diminishing epithelial barrier (2, 4, 10). These processes are also common to other atopic disorders. Pathologic epithelial remodeling responses and increased presence of inflammatory infiltrates and their activity are likely to increase the global metabolic demands on the esophageal epithelium in EoE, as has been observed in other chronic diseases (11). To date, no study has examined the role of microenvironmental oxygen metabolism and hypoxia in the pathogenesis of esophageal epithelial barrier dysfunction in EoE.

Mucosal surfaces dynamically regulate epithelial barrier function despite continuous exposures to toxic, infectious, and allergic molecules. In order to maintain this structural interface with the external environment, a number of innate and endogenous systems exist. One vital aspect of this functionality is cellular metabolism and the availability of oxygen. Physiologically normal oxygen levels are unique to each tissue ("physioxia") and may be altered in response to tissue activities such as metabolism or disease (hypoxia; ref. 12). Evolutionary adaptation to a hypoxic tissue microenvironment is mediated by the transcription factor hypoxia-inducible factor (HIF). In several systems, elevated HIF has been shown to augment barrier pro-

Authorship note: JJL is deceased.
Conflict of interest: The authors have declared that no conflict of interest exists.
Role of funding source: The study sponsors were not involved in the experimental design, interpretation of results, or preparation of this article.

Submitted: January 29, 2019; **Accepted:** May 16, 2019; **Published:** July 2, 2019.
Reference information: *J Clin Invest*. 2019;129(8):3224–3235.
https://doi.org/10.1172/JCI126744.

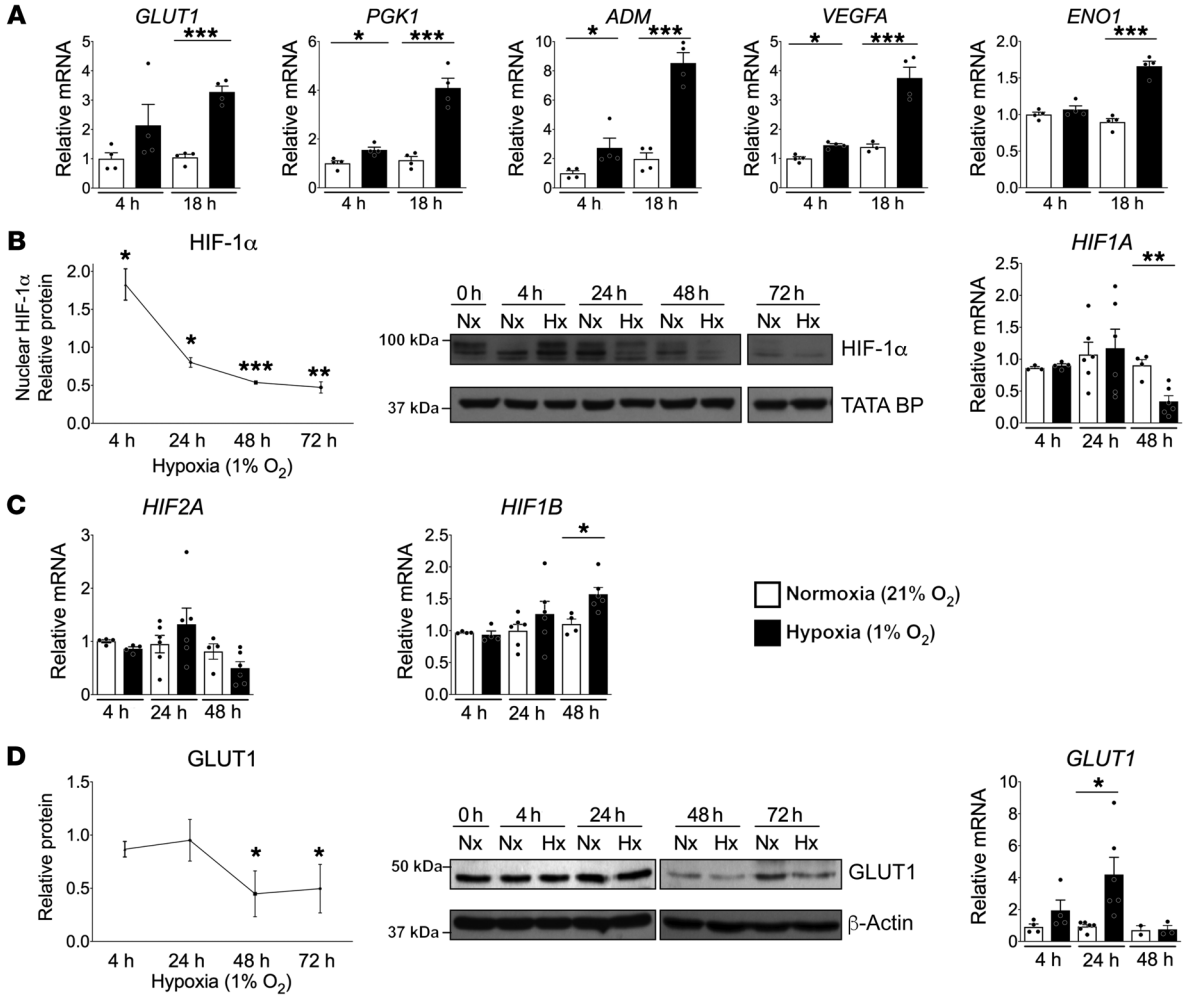

Figure 1. Prolonged experimental hypoxia results in attenuated HIF signaling in esophageal epithelial cells in vitro. (**A**) Short-term experimental hypoxic cultures induce elevated expression of HIF target genes. (**B**) HIF-1α expression was assessed by Western blot of nuclear protein lysate from esophageal epithelial cells exposed to a time course (0, 4, 24, 48, 72 hours) of experimental hypoxia compared with duration-matched normoxic cells and quantified by densitometry. (**B** and **C**) mRNA expression of *HIF1A* (**B**), *HIF2A*, and *HIF1B* (**C**) was assessed by real-time RT-PCR in cells exposed to a time course (4, 24, 48 hours) of experimental hypoxia compared with duration-matched normoxic cells. (**D**) Known HIF signaling target GLUT1 protein was assessed by Western blot in whole-cell protein lysates from esophageal epithelial cells exposed to a time course (0, 4, 24, 48, 72 hours) of experimental hypoxia compared with duration-matched normoxic cells and quantified by densitometry. mRNA expression of *GLUT1* was assessed by real-time RT-PCR in cells exposed to a time course (4, 24, 48 hours) of experimental hypoxia compared with duration-matched normoxic cells. For Western blots, a representative actin and a set of blots for a single time course are presented. Statistical significance was assessed using Students' *t* test comparing time point–matched normoxic controls with hypoxic samples. $^*P < 0.05$, $^{**}P < 0.01$, $^{***}P < 0.001$ (n = 3–6 per group). Data are presented as means ± SEM and represent a minimum of 3 experimental repeats.

tection. In this regard, we have previously established HIF's roles in mucosal protective functions regulating the expression of epithelial trefoil factor, mucin 3, and antimicrobial defensin, and, more recently, HIF-1α's regulation of tight junctions in T84 colon cancer cells (13–16).

In this study, we hypothesized that HIF signaling is dysregulated, contributing to barrier dysfunction in the allergic esophageal inflammatory disease EoE. Using in vitro and in vivo model systems with a recapitulation of esophageal epithelial changes in EoE, we sought to evaluate the potential contribution of HIF to the stratified squamous esophageal epithelial barrier dysfunction and investigate HIF's potential use as a treatment modality focused on mucosal healing and the reestablishment of epithelial barrier in allergic disease.

Results

Prolonged hypoxia leads to the suppression of HIF-1α signaling in esophageal epithelial cells. We first confirmed that esophageal epithelial cells were hypoxia responsive and screened a number of HIF target genes following short-term exposure to hypoxic cultures (4 and 18 hours) (Figure 1A). Here we observed increased expression of a number of known target genes, including *PGK1*, *ADM*, and *VEGFA*, following a short 4-hour hypoxic culture. Interestingly, both *GLUT1* and *ENO1* were increased at 4 hours but only reached statistical significance at 18 hours, suggesting there may be temporally distinct transcriptional regulation by HIFs in esophageal epithelial cells. We hypothesized that decreased HIF-1α signaling may be the result of prolonged hypoxic constraints on the esophageal epithelium in EoE-associated inflammation and contribute to barrier dys-

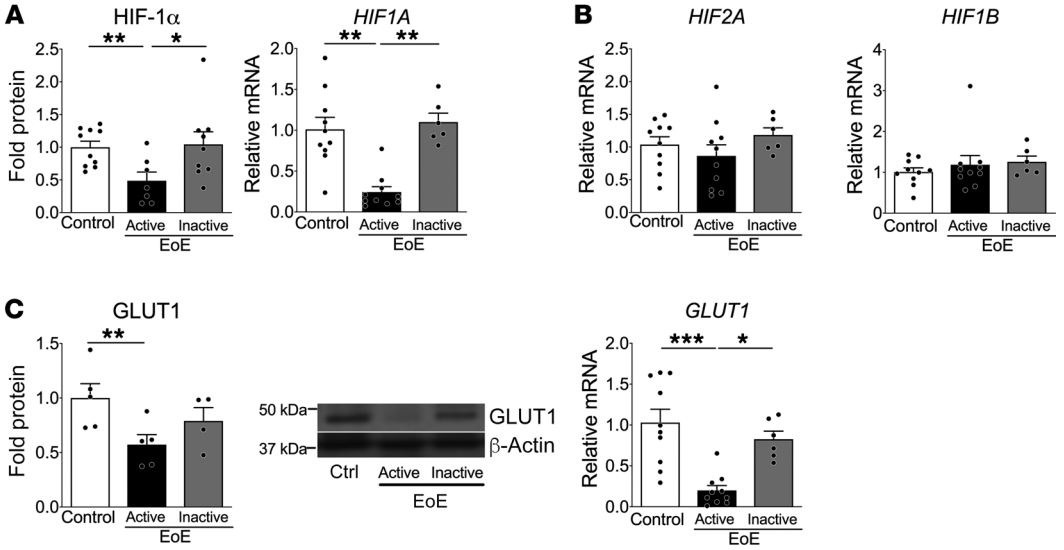

Figure 2. HIF signaling is dysregulated in patients with active EoE. Whole esophageal pinch biopsies from patients undergoing endoscopy were obtained for molecular analysis. (**A**) HIF-1α protein was assessed by mesoscale assay, and *HIF1A* mRNA transcript expression was assessed by real-time RT-PCR. (**B**) *HIF2A* and *HIF1B* mRNA transcript expression was assessed by real-time RT-PCR and compared between active disease, inactive disease, and control subjects. (**C**) Known HIF signaling pathway target GLUT1 protein was assessed by Western blot and quantified by densitometry, and mRNA transcript expression was assessed by real-time RT-PCR and also compared between active disease, control subjects, and those with inactive disease. Statistical significance was assessed using the nonparametric Kruskal-Wallis test with Dunn's correction for multiple comparisons. $^*P < 0.05$, $^{**}P < 0.01$, and $^{***}P < 0.001$ (mean ± SEM, n = 5–10 per group).

function. We examined HIF-1α protein expression in esophageal epithelial cells exposed to experimental hypoxia (1% O_2) compared with normoxic (21% O_2) cultures over a sustained period. Nuclear HIF-1α expression was transiently and significantly elevated in cultured esophageal epithelial cells (4 hours). However, this normalized by 24 hours, and following sustained hypoxic culture there was a significant decrease in nuclear HIF-1α protein (Figure 1B). *HIF1A* mRNA expression was also decreased following prolonged hypoxia (Figure 1B), with no observed effect on *HIF2A* or *HIF1B* (Figure 1C). To confirm the downstream consequences of HIF-1α suppression by sustained hypoxia, the expression of the well-known HIF target gene *GLUT1* was examined, and protein levels were not changed at 4 or 24 hours after hypoxia; however, coincident with decreased HIF-1α, by 48 hours a decrease in protein and mRNA expression, mirroring HIF-1α, was observed (Figure 1D).

HIF-1α signaling is attenuated in patients with ongoing active EoE. To understand the potential role of the transcription factor HIF-1α in chronic allergic esophageal inflammation, we tested whether expression was altered in patients with EoE. We examined protein and mRNA HIF-1α expression in whole esophageal biopsies from patients with active EoE compared with controls and patients with inactive EoE and found a specific decrease in comparison with control subjects (Figure 2A). No change in mRNA expression of *HIF2A* or the cotranscriptional unit *HIF1B* was observed in active EoE (Figure 2B). To examine effects of attenuated HIF-1α on downstream signaling, a significant decrease of the HIF target gene *GLUT1* at the protein and mRNA levels was confirmed in active EoE subjects compared with controls and inactive EoE (Figure 2C). These data implicate a potential role for dysregulated epithelial HIF signaling in the pathogenesis of EoE, likely not in the initiation, and led us to investigate the functional consequences of decreased esophageal epithelial HIF-1α.

Diminished HIF-1α signaling in physioxic esophageal epithelial cells leads to barrier dysfunction. To assess the functional consequences of diminished HIF-1α signaling in physioxic (physiologically normal oxygen) esophageal epithelial cells, we generated *HIF1A*-knockdown cells (*HIF1A*-KD) using shRNA technologies and confirmed approximately 90% protein depletion. To confirm the effects observed in these cells, we directly compared observations in 2 independent cell lines deficient in HIF-1α, comparing our generated *HIF1A*-KD cells with cells overexpressing a *HIF1A* that is deficient in HIF-1α transcriptional activity (*HIF1A*-DN). In a physiologically relevant, 3D air-liquid interface (ALI) model, barrier function in *HIF1A*-KD compared with shRNA control cells was assessed. Transepithelial electrical resistance (TEER) was significantly decreased (Figure 3A) and FITC flux was increased in *HIF1A*-KD cells (Figure 3A). To verify these findings, barrier and permeability in *HIF1A*-DN cells was assessed, and similar results were found, with increased paracellular permeability (FITC flux); however, the less sensitive, and differentially regulated, transcellular ion transport (TEER) was decreased (15%; $P = 0.3$), but not to a statistically significant degree (Figure 3B). This may reflect the differential regulation of ion transport and paracellular transport by HIF-1α in esophageal epithelial cells, or it could reflect the low sensitivity of the TEER resistance method compared with the paracellular FITC flux method.

Loss of basal HIF-1α signaling results in a specific decrease in claudin-1 expression. To test the molecular mechanisms through which this epithelial barrier functional deficit occurs, we performed a targeted array analysis of transmembrane cell-cell adhesion molecules using both *HIF1A*-KD and *HIF1A*-DN cells and focusing specifically on molecules concomitantly altered in both lines. We first noted that normal human esophageal biopsies possess the primary claudin genes *CLDN1*, *CLDN4*, and *CLDN7* (Figure 3C). We

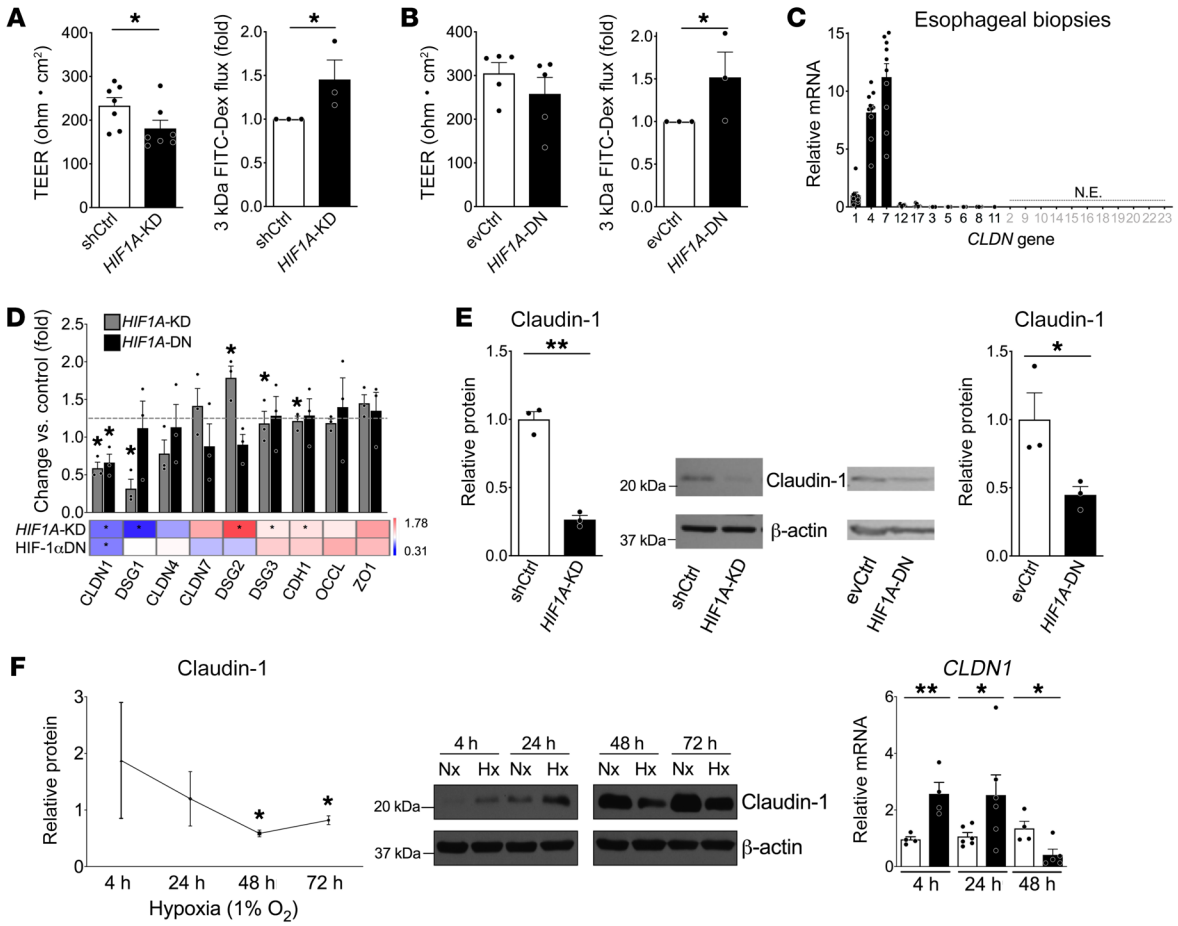

Figure 3. HIF-1α attenuation mediates esophageal epithelial barrier dysfunction and diminishes claudin-1 expression. (**A** and **B**) Esophageal epithelial cell lines were generated by shRNA-mediated HIF-1α suppression (*HIF1A*-KD) (**A**) and overexpression of a transcriptionally inactive dominant-negative HIF-1α variant (*HIF1A*-DN) (**B**). These cells and respective controls (scrambled shRNA [shCtrl] or empty vector [evCtrl]) were grown at ALI, and epithelial barrier (TEER) ($n = 3$) and paracellular permeability (3-kDa FITC-dextran flux) were measured in vitro ($n = 5$–7). (**C**) Patients' endoscopic esophageal pinch biopsies were assessed for mRNA expression of an array of claudin genes ($n = 10$). (**D**) *HIF1A*-KD and *HIF1A*-DN cells were examined for the expression of transmembrane junctional molecules. The dashed line represents control cells normalized to 1-fold. Heatmaps generated from normalized data ($n = 3$). (**E**) Western blotting confirmed claudin-1 protein loss in *HIF1A*-KD and *HIF1A*-DN cells, quantified by densitometry ($n = 3$). (**F**) Esophageal epithelial cells exposed to a time course (4, 24, 48, 72 hours) of experimental hypoxia compared with duration-matched normoxic cells were assessed for claudin-1 protein by Western blot in whole-cell lysates, and *CLDN1* mRNA by real-time RT-PCR ($n = 3$–6). Statistical significance was assessed using Students' *t* test. $^*P < 0.05$, $^{**}P < 0.01$. Data are expressed as means ± SEM and represent a minimum of 3 experiments.

next assessed their mRNA expression in *HIF1A*-KD and *HIF1A*-DN cells cultured at ALI and observed a significant and selective decrease in the tight junction molecule *CLDN1* (Figure 3D). We confirmed this specific claudin-1 effect at the protein level in both cell lines targeted for HIF-1α suppression (Figure 3E). In addition, we confirmed the *CLDN1*-specific decrease in *HIF1A*-KD epithelial cells grown in independent submerged cultures (*CLDN1*, 56% decrease, $P < 0.01$; *CLDN4* and *CLDN7*, NS). Significant changes in desmoglein and cadherin molecules were observed in *HIF1A*-KD cells that were not observed in *HIF1A*-DN cells, and thus were not pursued further in these studies. Together these data suggest that basal HIF-1α expression is integral to esophageal barrier function and mediates it in part by controlling claudin-1 expression.

Prolonged hypoxia leads to decreased CLDN1 expression in esophageal epithelial cells. Given the suppression of HIF-1α signaling in the context of prolonged hypoxia and the relationship between HIF-1α and *CLDN1*, we assessed the effects of prolonged hypoxia on *CLDN1* expression in esophageal epithelial cell cultures. A significant decrease in the expression of claudin-1 protein in cells in sustained hypoxia compared with time point–matched normoxic controls was detected, and this was confirmed by mRNA (Figure 3F). Together, these data support the distinguishing hypothesis that prolonged or sustained hypoxia in the esophageal epithelium leads to suppressed HIF-1α and decreased claudin-1 expression, and we suggest that this may occur in part through the dysregulation of HIF-1α–mediated *CLDN1* expression and that it underlies the development of barrier dysfunction in EoE pathogenesis.

ChIP analysis confirmed CLDN1 as a direct HIF-1α target gene in stratified squamous esophageal epithelia. We next examined whether *CLDN1* was a direct HIF-1α target gene in esophageal epithelial cells. First using chromatin immunoprecipitation (ChIP), we examined HIF-1α's capacity to bind to the *CLDN1* gene promoter. We identified 2 hypoxia-responsive elements (HREs) 224 bp and 588 bp upstream of the *CLDN1* transcription start site. We observed signif-

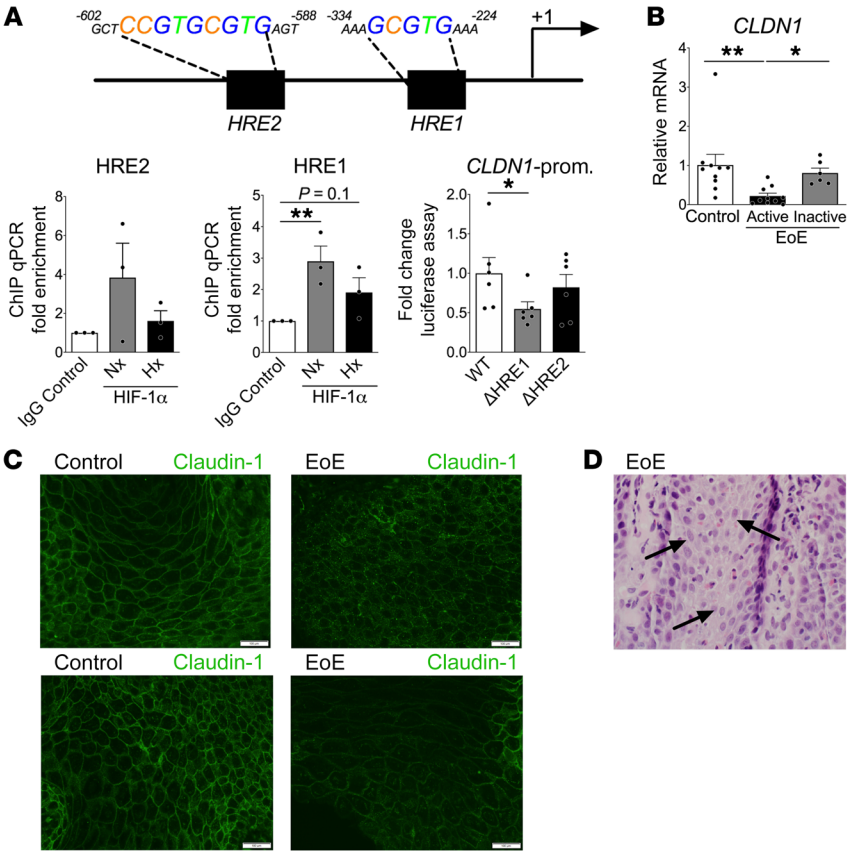

Figure 4. CLDN1 is a direct HIF-1α target gene, and claudin-1 protein is mislocalized in active EoE patients. (**A**) Proximal human *CLDN1* promoter sequence identified 2 potential hypoxia-responsive elements (HREs). Transcription start site, +1. ChIP using a HIF-1α antibody on cells exposed to 4 hours of hypoxia compared with normoxia, followed by PCR using primers spanning HRE2 and HRE1 sites, was normalized to PCRs performed on ChIP product generated using an isotype IgG control antibody (n = 3). Luciferase activity in lysates transfected with full-length *CLDN1* promoter (WT) compared with cells transfected with either mutated HRE site 1 or mutated HRE site 2. Luciferase data normalized to total cell protein content (n = 6). Statistical significance was assessed using an ordinary 1-way ANOVA with correction for multiple comparisons. $^*P < 0.05$, $^{**}P < 0.01$. (**B**) Esophageal pinch biopsies from patients undergoing endoscopy were obtained and assessed for *CLDN1* expression by real-time RT-PCR (n = 6–10 per group). Statistical significance was assessed using the nonparametric Kruskal-Wallis test with correction for multiple comparisons. $^*P < 0.05$, $^{**}P < 0.01$. (**C**) Representative photomicrographs of claudin-1 immunolocalization. Scale bars: 100 μm. (**D**) Arrows depict dilated intercellular spaces in H&E-stained FFPE pinch biopsies from active EoE subjects compared with normal controls. Data are expressed as means ± SEM and represent a minimum of 3 experimental repeats.

icant enrichment for HIF-1α binding to the most proximal HRE1^{-224} (Figure 4A). We tested the specificity of this response by constructing HRE site mutants and assessing *CLDN1*-LUC promoter reporter construct activation. Consistent with the importance of the HRE1 site in ChIP, *CLDN1*-LUC expression was significantly decreased in the HRE1 site mutant (Figure 4A). These data confirm the importance of direct HIF-1α transcriptional activation of *CLDN1*, specifically through the *CLDN1* promoter HRE1 site.

CLDN1 expression is attenuated and claudin-1 protein is mislocalized in patients with EoE. To determine the clinical relevance of these findings, we measured HIF-1α/claudin-1 in human esophageal biopsies. *CLDN1* mRNA was significantly decreased in active EoE compared with those with inactive disease and normal controls (Figure 4B). Immunohistochemical staining identified changes in claudin-1 protein pattern in comparison with normal tissues. Instead of the typical "chicken wire," membrane pattern, EoE tissues were found to have decreased cell membrane expression (Figure 4C) that corresponded to areas of dilated intercellular spaces observed in H&E-stained tissues (Figure 4D).

Prolonged and sustained hypoxia mediated by chronic esophageal epithelial eosinophilia leads to dysregulated HIF-1α/CLDN1 signaling axis in an experimental mouse model of EoE. We next hypothesized that one contributor to esophageal hypoxia during EoE-associated inflammation were eosinophils themselves. We developed a mouse model of EoE (L2-IL5^{OXA}) that results in significant esophageal eosinophilia, and by using major basic protein (MBP) immunohistochemistry we could identify eosinophils located throughout and intimately in contact with the epithelium, in addition to lamina propria (ref. 17 and Figure 5A). Colocalization of Hypoxyprobe-1$^+$ hypoxic tissue staining with eosinophilia (Siglec-F) in the esophageal epithelium in L2-IL5^{OXA} EoE mice was evident (Figure 5A). In vitro activated human eosinophils were capable of rapidly consuming oxygen (pO_2 measurements) from their local microenvironment when compared with nonactivated eosinophils (Figure 5A). To assess the effects of eosinophilic inflammation on tissue hypoxia in L2-IL5^{OXA} EoE mice, we measured the area of Hypoxyprobe-1$^+$ esophageal tissue. We elucidated a significant increase in the esophageal epithelium under hypoxic constraints compared with uninflamed WT^{OXA} controls (Figure 5B). These findings implicate activated eosinophils and their chronic esophageal epithelial infiltration in the sustained hypoxic burden on the esophageal epithelium during EoE.

Consistent with in vitro (Figure 1) and human subject (Figure 2) data, a significant decrease in HIF-1α signaling was observed in the L2-IL5^{OXA} EoE mouse. Western blotting confirmed decreased HIF-1α protein and attenuated HIF activity using ODD-LUC HIF-reporter-L2-IL5^{OXA} EoE mice compared with controls (ODD-LUC HIF-reporter-WT^{OXA}). Congruent with active clinical EoE specimens, decreased *HIF1A* mRNA and downstream signaling through the known HIF target gene *GLUT1* were confirmed (Figure 5C). The L2-IL5^{OXA} EoE mice exhibited elevated histologic activity, including significant intraepithelial eosinophilic inflammation, dilated intracellular spaces, and basal cell hyperplasia (Figure 5D). Consistent with clinical EoE, a significant decrease in EoE mouse esophageal *CLDN1* mRNA and protein was observed (Figure 5E). These data support our hypothesis that the HIF-1α/

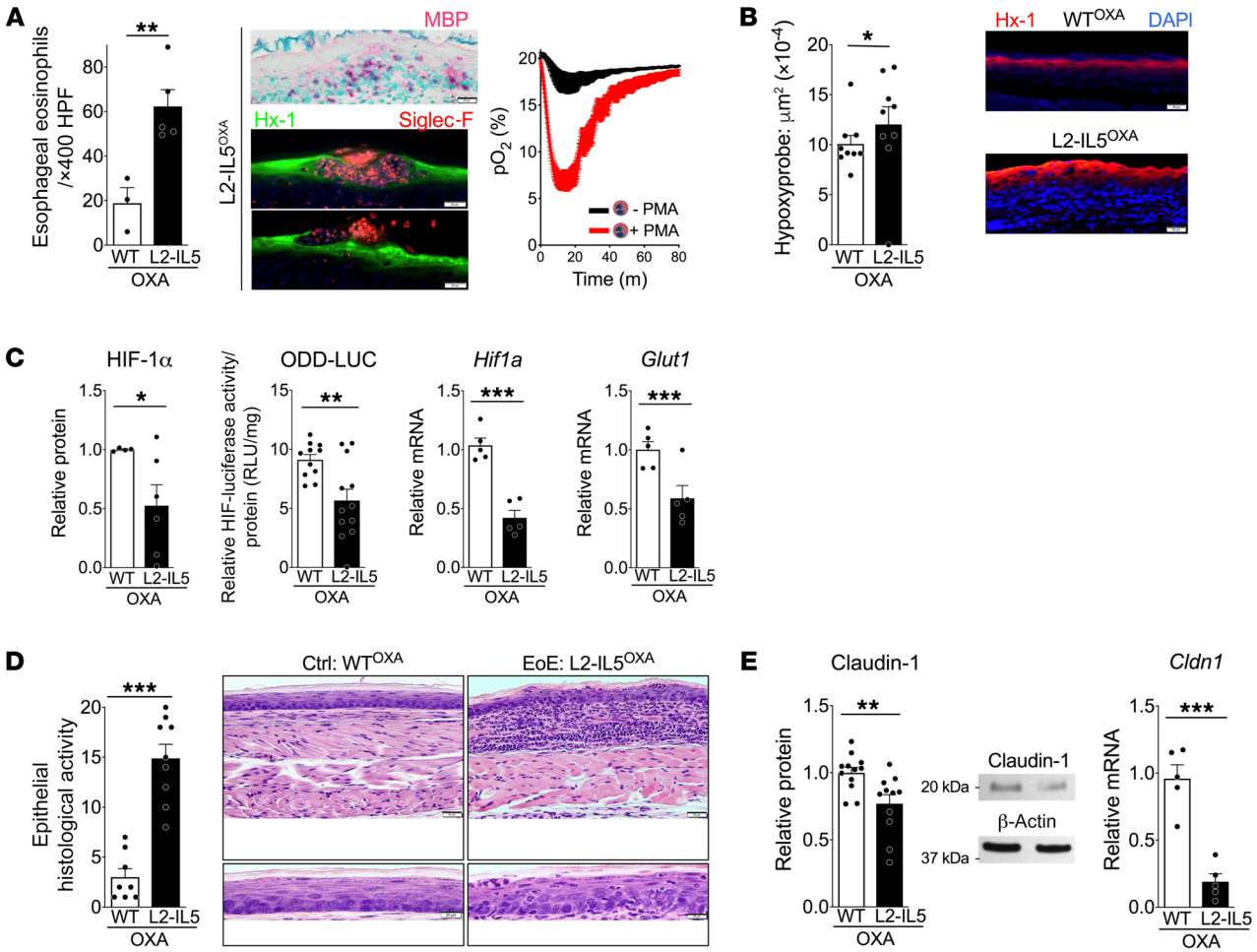

Figure 5. Prolonged and sustained hypoxia mediated by esophageal eosinophilia in experimental EoE leads to a dysregulated HIF-1α/CLDN1 signaling axis. (**A**) L2-IL5 transgenic mice and WT littermate controls were exposed to OXA-induced esophagitis and assessed for esophageal eosinophils using MBP immunohistochemistry or immunofluorescence for Siglec-F in conjunction with Hypoxyprobe-1 (Hx-1) (n = 3–9). Eosinophils were enumerated based on MBP staining per high-power field (HPF). Primary peripheral blood human eosinophils were isolated and stimulated in the presence or absence of PMA and assessed for oxygen consumption over time (minutes) (n = 3). Scale bars: 20 μm. (**B**) L2-IL5 transgenic mice and WT littermate controls were exposed to OXA-induced esophagitis and assessed for tissue oxygen tension by Hypoxyprobe-1 (Hx-1) immunofluorescent staining, which was quantified to measure the area of tissue under hypoxic constraints (n = 9 per group). Scale bars: 50 μm. (**C**) Whole esophageal tissues from OXA-challenged L2-IL5 and WT littermate control mice were assessed for HIF-1α protein expression by Western blot and quantified by densitometry (n = 4–6). WT ODD-LUC and L2-IL5/ODD-LUC luciferase reporter mice were challenged with OXA-induced esophagitis and assessed by luciferase assay for HIF/luciferase activity relative to total tissue protein (n = 12). OXA-challenged L2-IL5 and WT littermate control mice were assessed for *HIF1A* and *GLUT1* mRNA expression by real-time RT-PCR (n = 5). (**D**) OXA-challenged L2-IL5 and WT littermate control mice were assessed for histologic activity scores from H&E-stained esophageal tissues (n = 8–9). Scale bars: 50 μm (top); 20 μm (bottom). (**E**) Whole esophageal tissues were assessed for claudin-1 protein by Western blot and quantified by densitometry (n = 11), and were assessed for *CLDN1* mRNA transcript expression by real-time RT-PCR (n = 5). Representative blot is presented. Statistical significance was assessed using Students' t test. $^*P < 0.05$, $^{**}P < 0.01$, $^{***}P < 0.001$. Data are expressed as means ± SEM and represent a minimum of 3 experimental repeats.

claudin-1 axis is dysregulated in EoE in response to chronic esophageal inflammation, and support the utility of the L2-IL5^{OXA} EoE mouse in examining mechanisms of barrier dysfunction.

Conditional HIF-1α overexpression is protective in an EoE mouse model, and pharmacologic stabilization in human biopsies restores the HIF-1α/CLDN1 axis. Based on these findings, we speculated that HIF-1α stabilization might serve as a novel therapeutic intervention for EoE barrier dysfunction. To begin to address this, the L2-IL5^{OXA} mouse EoE model was genetically modified to selectively overexpress HIF-1α in the esophageal epithelium. Here, mutated, non–oxygen-sensitive, and thus less degradable HIF-1α was overexpressed specifically in the esophageal epithelium using the cytokeratin/K14 promoter, crossed with the L2-IL5 mouse (*K14Cre/LSL-HIF1A-dPA/L2-IL5*). *K14Cre/LSL-HIF1A-dPA/L2-IL5^{OXA}* mice experienced significantly attenuated epithelial histologic activity scores and eosinophilic inflammation compared with inflamed K14Cre-negative (*K14Cre$^-$*) EoE controls (Figure 6A). Furthermore, claudin-1 protein and mRNA were significantly increased in comparison with inflamed *K14Cre$^-$* EoE controls (Figure 6B). Confirming that this was associated with HIF-1α activity, increased expression of HIF target genes was observed in both *K14Cre$^+$* non–OXA-challenged and *K14Cre$^+$* OXA-challenged mice compared with *K14Cre$^-$* controls (Table 1). Taking a pharmacologic approach in vitro, the pan-hydroxylase inhibitor dimethyloxalylglycine (DMOG) was used to stabilize HIF. Consistent with reports in other cells, esophageal epithelial cells exposed to DMOG showed increased *GLUT1* and

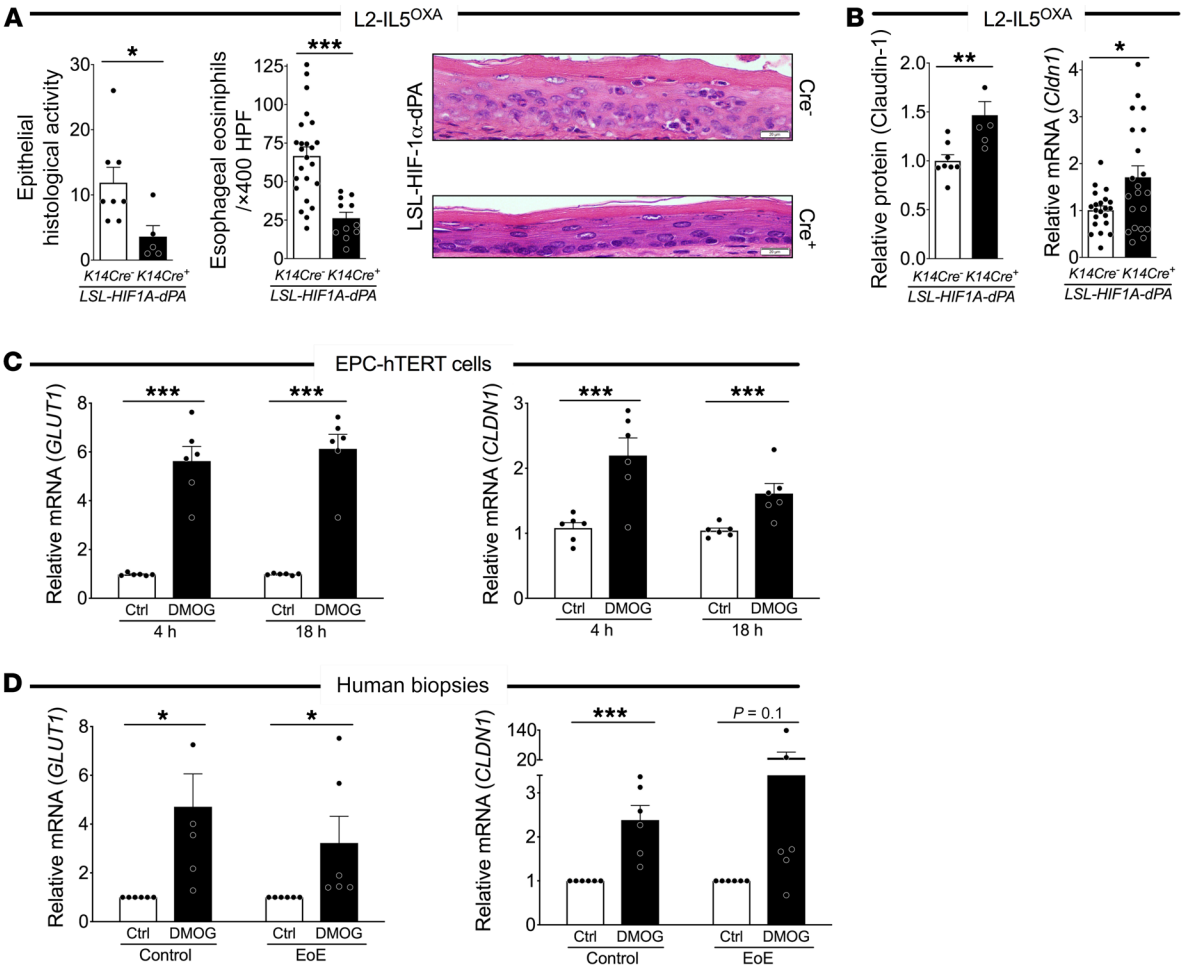

Figure 6. Genetic and pharmacologic stabilization of esophageal epithelial HIF-1α attenuates inflammation and barrier dysfunction in a mouse model of EoE via claudin-1 restoration. (**A**) Triple-transgenic *L2-IL5*$^{+}$*/LSL-HIF1A-dPA*$^{+/+}$*/K14Cre*$^{+}$ and *Cre*$^{-}$ control mice were exposed to OXA-induced esophagitis (n = 5–21) and assessed for histologic activity scores from H&E-stained tissues. Esophageal eosinophils were assessed using MBP immunohistochemistry and enumerated by MBP^{+} staining per HPF. Representative H&E photomicrographs. Scale bars: 20 μm. (**B**) Mice were assessed for claudin-1 protein by Western blot, quantified by densitometry, and *CLDN1* mRNA by real-time RT-PCR. (**C**) *GLUT1* and *CLDN1* mRNA were assessed by real-time RT-PCR in cells exposed to DMOG (1 mM) over a time course (4, 18 hours) (n = 6). (**D**) Patients' endoscopic esophageal pinch biopsies were obtained and treated ex vivo with DMOG (500 μM) for 24 hours. Biopsies were harvested and assessed for *GLUT1* and *CLDN1* mRNA by real-time RT-PCR (n = 6). Statistical significance was assessed using Students' t test. *P < 0.05, **P < 0.01, ***P < 0.001. Data are expressed as means ± SEM and represent a minimum of 3 experiments.

CLDN1 expression at 4 and 18 hours (Figure 6C). To test clinical applicability, human esophageal biopsies were treated with DMOG ex vivo. Tissue biopsies from both controls and active EoE subjects treated ex vivo with DMOG showed significantly increased expression of *GLUT1* and *CLDN1* (Figure 6D). Cumulatively, these data support the pursuit of HIF-1α–stabilizing therapies in addressing barrier dysfunction in EoE.

Discussion

In this study we report the striking decrease in esophageal expression of the transcription factor HIF-1α and its direct role in barrier dysfunction as a potentially novel pathophysiologic mechanism in the chronic allergic disease eosinophilic esophagitis (EoE). We demonstrate increased oxygen demands placed on the epithelial surface by eosinophilic inflammation and how chronic hypoxia contributes to maladaptive epithelial responses. Previous studies examining endogenous protective mechanisms of mucosal surfaces demonstrated a protective role for HIF-1α, a critical transcription factor in the adaptation to low oxygen tension (14–16). This study adds HIF-1α–focused therapies to the list of candidate treatments derived from endogenous protective mechanisms and directed at the maintenance and restoration of esophageal epithelial barrier and, furthermore, provides the foundation for extensive testing in other atopic conditions.

Previous work indicated, counter to expectations, that decreased HIF-1α is a result of prolonged experimental hypoxia in epidermal keratinocytes, endothelial cells, lung adenocarcinoma, and colon cancer cell lines in vitro (18–21). As observed in our control cells, nuclear HIF-1α may be augmented by the increasing confluence of cells in culture (22), and indeed this regulation may be cyclical, allowed for by nuclear-cytoplasmic shuttling (23). This regulation has been attributed to the actions of both prolyl hydroxylase–mediated protein degradation and microRNA-mediated mRNA degradation. Here we showed that while short cultures could induce nuclear HIF-1α accumulation and target gene expression, prolonged hypoxia in vitro resulted in esophageal

Table 1. *L2-IL5*$^{+}$*/LSL-HIF1A-dPA*$^{+/+}$*/K14Cre*$^{+}$ mice at baseline (Control) and during esophagitis (L2-IL5^{OXA}) compared relative to baseline Cre^{-} controls or vehicle-challenged (*n* = 5–6 per group)

Control

Fold change	Cre^{-} Ctrl	Cre^{+} dPA
GLUT1	1	1.1^{A}
PGK1	1	1.6^{C}
ADM	1	1.4^{A}

L2-IL5^{OXA}

Fold change	Cre^{-} Ctrl	Cre^{+} dPA
GLUT1	1	1.45^{A}
PGK1	1	1.72 (P = 0.08)
ADM	1	1.89^{B}

$^{A}P < 0.05$, $^{B}P < 0.01$, $^{C}P < 0.001$.

epithelial suppression of HIF-1α. We report a specific repression of the HIF-1α transcription factor distinct from any effects on *HIF2A* or *HIF1B* during sustained tissue hypoxia in the esophageal epithelium in both mouse and human studies. Notably, while we observed increased transcription of the HIF target gene *GLUT1*, no concomitant increase in *GLUT1* protein was observed. The regulation of *GLUT1* mRNA and protein is a complex process involving posttranslational and post-transcriptional events, and similar mRNA increases in the absence of protein have previously been reported (24, 25). Future detailed and focused studies may examine the regulation of *GLUT1* expression at these levels and, in addition, glucose affinity, membrane density, and distribution relative to protein half-life in esophageal epithelial cells. Eosinophil activation rapidly increased oxygen consumption consistent with neutrophils (26), suggesting that sustained esophageal infiltration of activated eosinophils would in part contribute to increased tissue oxygen demands. Supporting clinical relevance was demonstrated through decreased esophageal HIF-1α signaling in EoE patient specimens and confirmed by a concurrent decrease in the canonical HIF target gene *GLUT1* (27). The prolonged nature of the elevated hypoxia affecting the esophageal epithelium in EoE is supported by the finding that activated eosinophils consume oxygen from the local epithelial microenvironment and thus may contribute to long-lasting tonal increases in esophageal epithelial hypoxia, mediating HIF-1α suppression.

Tight junctions, adherens junctions, and desmosomes are crucial cell-cell junctions that support tissue integrity. Paracellular macromolecule movement and barrier function are mediated in part by the tissue-specific transmembrane claudin protein family. Their altered expression and cellular redistribution are key steps in certain pathophysiologies, and claudins are elegantly regulated and expressed in a tissue- and cell type–specific manner (28). Claudin-1 is a critical mediator of skin barrier (29). In the esophagus, claudin-1 is decreased in gastroesophageal reflux disease (GERD) (30) and EoE (31), is associated with increased spongiosis (32), and in one study was described as nonresponsive to corticosteroid therapy (8). In esophageal squamous cell carcinoma, claudins 1, 4, and 7 are also dysregulated, leading to invasion (33). Although previous studies described the esophageal expression of claudins 1, 4, and 7 (33), no previous assessment examined a larger panel of transmembrane junctional molecules in the healthy esophagus. In this screen of 23 claudin isoforms in the healthy human esophagus, we found claudins 1, 4, and 7 to be the most highly expressed. Furthermore, in 2 HIF-1α–deficient cell lines used in these studies, we found a specific and selective, structural and functional, relationship between HIF-1α and transcriptional regulation of claudin-1 not observed in any other junctions, adherens junctions, or desmosome members. Notably, no increase in other tight junction claudins (claudin-4 or -7), occludin, or zonula occludens-1 was observed in either *HIF1A*-KD or *HIF1A*-DN cells, despite this claudin-1–specific decrease. It is well appreciated that the regulation and interdependency or coregulation of the large family of claudin molecules is a diverse, complex, and often redundant process that is cell type and organ specific during development and homeostasis, in addition to the responses to microenvironmental cues such as inflammation or indeed hypoxia (34, 35). We cannot exclude in totality potential indirect effects of *CLDN1* suppression itself on other junctional molecules; however, our data support the utility of genetically and pharmacologically targeting HIF-1α to mediate attenuated esophageal inflammation in conjunction with increased claudin-1 expression in both mouse and human studies. We previously reported a decrease in esophageal claudin-7 in EoE patients in response to TGF-β1 (36). We demonstrate here that decreased claudin-7 is not mediated by HIF-1α; however, together these studies now propose multiple and independent pathophysiologic mechanisms uniquely targeting each of 2 tight junction claudins in EoE. Accordingly, the HIF-1α isoform appears to play a key selective role in esophageal barrier function by mediating the expression of *CLDN1*, and both are decreased in active human EoE and the L2-IL5^{OXA} EoE mouse model. Given the fundamental importance of barrier in atopy, our findings presented in these studies also have implications in the broader field of atopic diseases.

It is well recognized that the healthy skin is hypoxic (37) and that HIF-1α signaling is important for wound revascularization, cellular migration, and wound closure (38, 39). In contrast, HIF-2α signaling can delay skin wound healing (40), suggesting opposing roles for these 2 isoforms in the skin. HIF-1α signaling is favorable for keloid-derived keratinocyte epithelial-mesenchymal transition (41) and epidermal carcinogenesis (42). Hypoxia can enhance proliferation and migration of skin outer root sheath cells (43). Other esophageal studies have characterized HIF-1α and HIF-2α expression as prognostic biomarkers in GERD (44) and progression of Barrett's esophagus to esophageal adenocarcinoma (45), while increased HIF-2α is thought to participate in mediating inflammation in GERD (44). This study focuses on the chronic allergic esophageal disease EoE and is, to our knowledge, the first study using a staining approach to show that, like the normal skin, the physiologically healthy esophagus is hypoxic. Decreased *HIF1A* mRNA expression has recently been associated with food impactions in EoE patients during a transcriptomics study (46). To our knowledge, ours is the first study to mechanistically dissect the role of HIF-1α in esophageal epithelial function and in the context of mucosal healing in EoE.

With the exception of topical barrier creams/emulsions in atopic dermatitis, no current atopic disease therapy directly targets the mucosa for endogenous healing mechanisms and epithelial barrier restoration. Current therapies for EoE are limited to dietary exclusion of food allergens, swallowed topical steroids, or endoscopic dilation, each of which can impact quality of life, involve poor adherence/compliance, and have potential side effects (47). An important recent study highlighted the continued absence of junctional proteins in patients with EoE despite corticosteroid treatment being effective in reducing innate immune mechanisms (8). Thus, a therapy focused on augmenting barrier, and possibly independent of immune effects, would be of significant importance for EoE. In order to address the need for alternative therapeutic options, we sought to understand the potential role for the transcription factor HIF-1α in esophageal epithelial mucosal healing and barrier. In these studies we identified a specific decrease in esophageal HIF-1α expression in EoE, while, interestingly, HIF-2α remained unchanged. Thus, these studies have elucidated unique epithelial cell responses to esophageal inflammation in a disease context–dependent manner and support the development of HIF-1α–specific targeting therapies for EoE.

In these studies, the HIF-stabilizing pan-PHD inhibitor DMOG was used, which may mediate effects on all isoforms. Reinforcing the translational relevance, we observed increased claudin-1 expression in vitro in epithelial cells and ex vivo in human explant biopsy tissues cultured with DMOG. In support of these findings, previous functional studies with colon adenocarcinoma cells found that PHD inhibition decreased IFN-γ–induced barrier dysfunction (48). Complications related to systemic PHD inhibition involving multicellular effects, including circulating eosinophils, and difficulty in obtaining HIF-1α–selective compounds, led to the development of a selective genetic approach in vivo to generate a Cre-flox transgenic mouse that overexpressed HIF-1α in the esophageal epithelium. Having overcome HIF isoform and epithelial cell specificity, we uncovered a striking and significant attenuation of inflammation and the restoration of claudin-1 expression in EoE mice. Thus, we can conclude that epithelial-specific attenuation of claudin-1 by HIF-1α contributes to inflammation, highlighting the need for future studies focusing on localized delivery of innovative HIF-1α–specific therapeutics.

In conclusion, we believe these studies establish a novel and crucial role for the hypoxia-associated transcription factor HIF-1α in the regulation of stratified squamous epithelial responses during allergic esophageal inflammation. Eosinophil infiltration into the physioxic esophagus leads to a sustained increase in oxygen consumption, tissue hypoxia, HIF-1α suppression, decreased claudin-1, and barrier disruption. Using genetic and pharmacologic approaches, these studies provide a mechanistic explanation for the beneficial effects of the restoration of oxygen-metabolism signaling and highlight an innovative therapeutic modality for selective HIF-1α targeting as a useful mechanism to restore epithelial barrier and in mucosal healing for patients with allergic esophageal inflammation and EoE.

Methods

Human subjects. Subjects aged 2–20 years from Children's Hospital Colorado who underwent clinically indicated endoscopy and esophageal mucosal biopsy were included in these studies. Based on review of the clinical record, subjects were subdivided into normal controls, EoE-active, and EoE-inactive. Subjects were defined as follows: (a) Control subjects had symptoms including abdominal pain, feeding difficulty, poor weight gain, and diarrhea, were not found to have an underlying clinical cause, and had normal esophageal histology including 0 eosinophils per high-power field (HPF). (b) EoE-active subjects had symptoms of esophageal dysfunction including abdominal pain, dysphagia, feeding difficulty, poor weight gain, and vomiting and ≥15 eosinophils per HPF, and other causes for eosinophilia had been ruled out according to consensus recommendations (49). (c) EoE-inactive subjects had an established EoE diagnosis and underwent treatment with topical corticosteroids or dietary elimination with resolution of symptoms and fewer than 15 eosinophils per HPF. Clinical features recorded included clinicopathologic diagnosis, age, sex, and peak eosinophils per HPF (Table 2). Esophageal biopsies were either placed in 10% buffered formalin for paraffin embedding, sectioning, and H&E analysis or another set of biopsies were snap-frozen and stored at –80°C for molecular analysis as described. For ex vivo cultures, biopsies were placed in media containing the pan-hydroxylase inhibitor dimethyloxalylglycine (DMOG; 500 μM) for 24 hours and harvested for mRNA analysis.

Cell culture and 3D ALI culture. EPC2-hTERT, EPC2-hTERT-HIF-1αDN (DNA-binding domain deleted), and EPC2-hTERT-ev control immortalized human esophageal epithelial cells were generated and cultured routinely in keratinocyte serum-free media (KSFM; Thermo Fisher Scientific) as previously described (36, 50, 51).

Cellular responses to experimental hypoxia and to the pan-hydroxylase inhibitor (DMOG, 1 mM; Cayman Chemical) were assessed for mRNA (24-well) and protein (6-well) analysis. Twenty-four hours after plating, medium was replaced with preconditioned normoxic (21% O_2) or hypoxic (1% O_2) medium or with medium containing DMOG, and cells were placed in respective culture chambers for 0, 4, 18, 24, 48, or 72 hours for analysis.

For assessment of barrier and ChIP, cells were grown in a 3D air-liquid interface (ALI) culture system, previously described (7, 36). Briefly, cells were seeded onto 0.4-μm-pore-size polyester 6-well Transwell supports and grown to confluence (Corning Costar). Cells were placed in high-calcium KSFM ($[Ca^{2+}]$ = 1.8 mM) and cultured for 5 days at ALI to allow barrier to form. At this point cells were assessed for barrier function or harvested for mRNA, protein, or ChIP analysis. Barrier assessment was performed by 2 means, first using transepithelial electrical resistance (TEER) with an ohm meter (World Precision Instruments), and second assessing paracellular permeability using the highly sensitive 3-kDa FITC-dextran (3 kDa; Molecular Probes, Invitrogen) flux assays previously described (36). Cells were harvested in RLT buffer from Qiagen RNeasy kits for mRNA, RIPA buffer plus Roche cOmplete Mini Protease Inhibitor Cocktail (Sigma-Aldrich) for protein or for ChIP.

Chromatin immunoprecipitation. For ChIP, cells were exposed to normoxia or hypoxia for 5 hours and fixed in 1% formaldehyde for 10 minutes at 4°C. Cells were sonicated, and the resulting sheared chromatin was incubated with 5 μg of control goat IgG or goat anti–human HIF-1α antibody (NB100-134, Novus Biologicals) and ChIP performed per the manufacturer's instructions (Exacta-ChIP Kit, R&D Systems). Input DNA, beads, IgG, and DNA replicates enriched for HIF-1α binding were amplified by real-time reverse transcriptase PCR (RT-PCR) using *CLDN1* promoter HRE-spanning primers (Table 3).

Table 2. Patient demographics examined in RT-PCR, Mesoscale assay (MSD), Western blot, or DMOG ex vivo cultures

Biopsy set 1: RT-PCR (Ctrl = 10, EoE-active = 10, EoE-inactive = 6)

	Age	Male	Female	Peak eosinophils per high-power field
Ctrl	8.2 ± 1.3	50%	50%	0 ± 0
EoE-active	8.9 ± 1.7	60%	40%	46.5 ± 11
EoE-inactive	7.16 ± 1.6	33.3%	66.6%	2.16 ± 1.10

Biopsy set 2: MSD (Ctrl = 10, EoE-active = 8, EoE-inactive = 9)

	Age	Male	Female	Peak eosinophils per high-power field
Ctrl	11.4 ± 1.3	60%	40%	0 ± 0
EoE-active	9.5 ± 2	50%	50%	61.75 ± 11.5
EoE-inactive	7.1 ± 0.8	33.3%	66.6%	1.89 ± 0.82

Biopsy set 3: Western blot (Ctrl = 5, EoE-active = 5, EoE-inactive = 5)

	Age	Male	Female	Peak eosinophils per high-power field
Ctrl	10.4 ± 1.2	80%	50%	0 ± 0
EoE-active	10 ± 3.2	80%	20%	42 ± 9.6
EoE-inactive	10 ± 1.8	80%	20%	0 ± 0

Biopsy set 4: DMOG cultures ex vivo (Ctrl = 6, EoE = 6)

	Age	Male	Female	Peak eosinophils per high-power field
Ctrl	11.5 ± 2.3	17%	83%	0 ± 0
EoE	10.3 ± 2.7	67%	33%	71.5 ± 27.8

shRNA knockdown, promoter mutagenesis, transfections, and luciferase assay. For *HIF1A* knockdown in EPC2-hTERT cells, cells were transduced with *HIF1A*-targeting shRNAs incorporated into lentiviral particles (MISSION TRC shRNA, Sigma-Aldrich) for 24 hours before 0.3 μg/mL puromycin antibiotic selection. Nontargeting shRNA was used as a control (shCtrl). Knockdown was confirmed by Western blot analysis, indicating approximately 90% depletion of *HIF1A*.

CLDN1 promoter luciferase reporter construct (Switchgear Genomics) was mutated using the QuikChange Site-Directed Mutagenesis Kit previously described (ref. 13; Agilent) with primers directed against each HRE site (Figure 4A). Four hundred nanograms of the luciferase reporter plasmids *CLDN1*-WT-Luc, *CLDN1*-δHRE1-Luc, and *CLDN1*-δHRE2-Luc were transfected in 24-well dishes using Fugene reagent (Promega) per the manufacturer's instructions. Cells were harvested 48 hours after transfection and promoter luciferase activity measured using Lightswitch luciferase reagent (Switchgear Genomics) and normalized to total cell protein determined using Pierce BCA assay (Thermo Fisher Scientific).

Human eosinophil isolation. Human eosinophils were isolated from healthy volunteers. Briefly, white blood cells were isolated from whole blood and anticoagulated with 5% citrate buffer. Plasma was removed following centrifugation. Erythrocytes were pelleted from leukocytes using 6% dextran/0.9% saline sedimentation (Fluka). Granulocytes were isolated from discontinuous Percoll gradients (42% and 51%; Sigma-Aldrich) and monocytes discarded. Residual erythrocytes were lysed with ice-cold water, and the remaining cells washed. Eosinophils were purified by negative selection using anti-CD16 and anti-CD14 MACS microbeads and AutoMACS separation (Miltenyi Biotec). Eosinophils were more than 95% pure as assessed by 4% fast green. Freshly isolated eosinophils were cultured in 25 ng/mL IL-5 and assessed after culture in the presence or absence of 1 μM PMA (Sigma-Aldrich) for the 80-minute duration of the O_2 consumption assay. Real-time O_2 measurements were performed using Oxodish plates on an SDR reader (PreSens; ref. 26).

Mice. Studies were performed with male and female transgenic L2-IL5 mice (17) bred in house (C57BL/6J; Jackson 000664). ODD-LUC FVB.129S6-*Gt(ROSA)26Sor*$^{tm2(HIF1A/luc)Kael}$/J (ref. 52; Jackson 006206), K14-Cre Tg(KRT14-cre)1Amc/J (Jackson 004782), and LSL-HIF1A-dPA B6.129S6(C)-*Gt(ROSA)26Sor*$^{tm3(HIF1A*)Kael}$/J (Jackson 009673) mice were obtained from The Jackson Laboratory. L2-IL5/ODD-LUC double-transgenic mice were generated by crossing of ODD-LUC with L2-IL5 mice. L2-IL5–negative ODD-LUC mice were controls. Triple-transgenic mice were generated by crossing of K14-Cre mice with LSL-HIF1A-dPA mice and L2-IL5 mice (*L2-IL5*$^{+}$*/HIF-1α-dPA*$^{+/+}$*/K14Cre*$^{+}$). Cre-negative littermates were controls. Animals were maintained in microisolator specific pathogen–free housing at the University of Colorado. Age- and sex-matched littermate mice were experimental controls.

Induction of experimental EoE in L2-IL5^{OXA} *mice using OXA*. Induction of esophageal eosinophilia in mice carrying the L2-IL5 transgene (L2-IL5^{OXA} EoE) was established as previously described using a 4-ethoxymethylene-2-phenyl-2-oxazolin-5-one (oxazolone [OXA], Sigma-Aldrich) contact hypersensitivity protocol (17). Briefly, anesthetized mouse abdomens were shaved, and OXA was applied (3% [wt/vol] in 4:1 acetone/olive oil vehicle). Mice were challenged by an intraesophageal gavage of 2% (wt/vol) OXA in 30% ethanol/olive oil vehicle on days 5, 8, and 12. In some studies, 200 mg dexamethasone was administered on protocol days 5, 8, 10, and 12 by i.p. injection (Vedco; ref. 17). All mice were assessed 24 hours after the last challenge (protocol day 13), and esophagi were removed and processed. ODD-LUC mouse (52) esophageal tissues were sonicated and assessed for firefly luciferase activity using standard Dual Luciferase Assay Kit (Promega), with data standardized to total protein.

Immunofluorescence and immunohistochemical analysis. Patient mucosal pinch biopsies or whole-length mouse esophageal tissues were fixed with 10% neutral buffered formalin, processed, paraffin-embedded, cut into 5-μm sections, and either stained with H&E (Sigma-Aldrich) or subjected to immunohistochemistry for eosinophil major basic protein-1 (MBP-1; clone MT-14.7, Lee Labs, Mayo Clinic, Arizona, USA; refs. 17, 53) or immunofluorescence for human claudin-1 (polyclonal rabbit anti–claudin-1; 51-9000, Invitrogen) with appropriate Alexa Fluor (Invitrogen) secondary antibody, mouse Hypoxyprobe-1 (mouse FITC-Mab or mouse Dylight 549-Mab) (Hypoxyprobe Inc.), and mouse PE-labeled Siglec-F (BD Biosciences). MBP-1 was visualized with Permanent Red chemotrope (Dako) and counterstained with Methyl Green (Vector Laboratories). Immunofluorescence slides were counterstained with DAPI (Invitrogen). Quantification of MBP-1–immunopositive cells or Hypoxyprobe-1–positive tissue area was determined by gathering of the

Table 3. ChIP PCR primers

CLDN1 promoter	Forward	Reverse
HRE1	CCACGAGAGAAAGCGAGCAGGG	CGGTTTCAGGGCGGCTCACC
HRE2	GGTGTTTGGCGGGGAAGGG	CAGACACACTCACGCACGG

numerical averages of 9 nonoverlapping HPFs (0.26 mm^2) per mouse esophagus (3 distal, 3 mid, and 3 proximal) using a Nikon Eclipse Ti-S microscope and Nikon NIS-Elements software. Cell numbers and area are presented as mean ± SEM.

RNA isolation and real-time RT-PCR. Total RNA was prepared from human mucosal pinch biopsies, whole esophageal mouse tissues, or cultured cells with RNeasy Mini Kits (Qiagen), first-strand cDNA synthesis using the High Capacity cDNA archive kit (Applied Biosystems), and TaqMan Gene Expression Assays TaqMan probes in real-time RT-PCR reactions using TaqMan Fast Advanced Master Mix (Applied Biosystems). Thermocycling and analysis were performed with an ABI-7300 System and software, and data calculated as relative quantification were normalized to 18S ($2^{-\Delta\Delta Ct}$; refs. 17, 53).

Protein assessment in esophageal tissues and cell cultures. Whole-cell or whole-tissue protein was prepared using RIPA buffer containing 1× Roche cOmplete Mini Protease Inhibitor Cocktail and PMSF (Sigma-Aldrich). Nuclear lysates were isolated using NE-PER Nuclear Extraction Reagents per the manufacturer's instructions (Thermo Fisher Scientific) for HIF-1α protein. Total protein content was assessed using BCA Assay (Thermo Fisher Scientific). Western blot was performed using rabbit polyclonal anti-GLUT1 (ab652, Abcam), mouse monoclonal anti–HIF-1α (clone 54, BD Biosciences), rabbit polyclonal anti–claudin-1 (51-9000, Invitrogen), rabbit polyclonal anti–β-actin (A5060, Sigma-Aldrich), and mouse monoclonal TATA-binding protein (1TBP18, Abcam). HIF-1α Mesoscale Assay was performed on sonicated human biopsies per the manufacturer's instructions (Meso Scale Diagnostics).

Statistics. Data outcomes statistical analyses were performed using Mann-Whitney test, ordinary 1-way ANOVA, or Kruskal-Wallis tests with Bonferroni or Dunn's correction for multiple comparisons or correction by controlling of false discovery rate or Student's *t* test where appropriate. Data are expressed as means ± SEM. A *P* value less than or equal to 0.05 was considered statistically significant. In some cases higher levels of significance are noted; $^*P \le 0.05$, $^{**}P \le 0.01$, $^{***}P \le 0.001$.

Study approval. Studies involving animals were performed in accordance with NIH guidelines and with approval of animal care and use for these experiments by the IACUC of the University of Colorado.

Author contributions

JCM, SPC, and GTF were responsible for the study concept and design. JCM, KAB, JAH, NN, KEC, BJS, RFH, SDF, LBH, CJK, ELC, SFE, FNA, HN, and ENM acquired data.JCM, ENM, LEG, SPC, and GTF analyzed and interpreted the data. JCM, ENM, SPC, and GTF drafted the manuscript and provided critical revision and important intellectual content. JCM and GTF obtained funding for the study. JCM, JJL, LEG, SPC, and GTF supervised the study.

Acknowledgments

We thank the members of the participating laboratories and the members of the Gastrointestinal Eosinophilic Diseases Program, Children's Hospital Colorado, for insightful discussions and critical comments. We thank the physicians, nurses, research assistants, pathology staff, and endoscopy technical staff who contributed to this work by helping to provide and collect samples and recruit subjects. We are grateful to our patients and families who consented to be a part of this study. We also acknowledge the invaluable assistance in animal husbandry and care at the University of Colorado School of Medicine (Kristann Magee and Sarah Williams) and the administrative support provided by Joshua Rosenfeld. Grants from the NIH (K01-DK106315 to JCM; 1K24-DK100303 to GTF; R01-DK114436 and P30-DK050306 to HN), the American Partnership for Eosinophilic Disorders (to JCM), and the NIH Consortium of Eosinophilic Gastrointestinal Disease Researchers (CEGIR; to GTF) were sources of funding used in the performance of studies, including data analysis and manuscript preparation. CEGIR (U54 AI117804) is part of the Rare Diseases Clinical Research Network, an initiative of the Office of Rare Diseases Research, National Center for Advancing Translational Sciences (NCATS), and is funded through collaboration between the National Institute of Allergy and Infectious Diseases, the National Institute of Diabetes and Digestive and Kidney Diseases, and NCATS. Article contents are the authors' sole responsibility and do not necessarily represent official NIH views. The study sponsors played no role in the study design or in the collection, analysis, and interpretation of data.

Address correspondence to: Joanne C. Masterson, Allergy, Inflammation and Remodeling Research Laboratory, Human Health Research Institute, Department of Biology, Maynooth University, Maynooth, County Kildare, Ireland. Phone: 353.1.708.6369; Email: joanne.masterson@mu.ie.

ELC's present address is: Wellcome-Wolfson Institute for Experimental Medicine, Queen's University Belfast, Belfast, Ireland.

SFE's present address is: Department of Anesthesiology and Intensive Care Medicine, University Hospital Bonn, Bonn, Germany.

1. Hill DA, Grundmeier RW, Ramos M, Spergel JM. Eosinophilic esophagitis is a late manifestation of the allergic march. *J Allergy Clin Immunol Pract*. 2018;6(5):1528–1533.
2. Blanchard C, et al. Coordinate interaction between IL-13 and epithelial differentiation cluster genes in eosinophilic esophagitis. *J Immunol*. 2010;184(7):4033–4041.
3. Kottyan LC, et al. Genome-wide association analysis of eosinophilic esophagitis provides insight into the tissue specificity of this allergic disease. *Nat Genet*. 2014;46(8):895–900.
4. Rochman M, Azouz NP, Rothenberg ME. Epithelial origin of eosinophilic esophagitis. *J Allergy Clin Immunol*. 2018;142(1):10–23.
5. Zeng C, et al. Solute carrier family 9, subfamily A, member 3 (SLC9A3)/sodium-hydrogen exchanger member 3 (NHE3) dysregulation and dilated intercellular spaces in patients with eosinophilic esophagitis. *J Allergy Clin Immunol*. 2018;142(6):1843–1855.
6. Capocelli KE, Fernando SD, Menard-Katcher C, Furuta GT, Masterson JC, Wartchow EP. Ultrastructural features of eosinophilic oesophagitis: impact of treatment on desmosomes. *J Clin Pathol*. 2015;68(1):51–56.
7. Sherrill JD, et al. Desmoglein-1 regulates esophageal epithelial barrier function and immune responses in eosinophilic esophagitis. *Mucosal Immunol*. 2014;7(3):718–729.
8. Simon D, et al. Evidence of an abnormal epithelial barrier in active, untreated and corticosteroid-treated eosinophilic esophagitis. *Allergy*. 2018;73(1):239–247.
9. Alexander JA, et al. Comparison of mucosal impedance measurements throughout the esophagus and mucosal eosinophil counts in endoscopic biopsy specimens in eosinophilic esophagitis. *Gastrointest Endosc*. 2019;89(4):693–700.e1.
10. Rochman M, Travers J, Abonia JP, Caldwell JM, Rothenberg ME. Synaptopodin is upregulated by IL-13 in eosinophilic esophagitis and regulates esophageal epithelial cell motility and barrier integrity. *JCI Insight*. 2017;2(20):96789.
11. Eltzschig HK, Carmeliet P. Hypoxia and inflam-

mation. *N Engl J Med*. 2011;364(7):656–665.
12. Carreau A, El Hafny-Rahbi B, Matejuk A, Grillon C, Kieda C. Why is the partial oxygen pressure of human tissues a crucial parameter? Small molecules and hypoxia. *J Cell Mol Med*. 2011;15(6):1239–1253.
13. Saeedi BJ, et al. HIF-dependent regulation of claudin-1 is central to intestinal epithelial tight junction integrity. *Mol Biol Cell*. 2015;26(12):2252–2262.
14. Kelly CJ, et al. Fundamental role for HIF-1α in constitutive expression of human β defensin-1. *Mucosal Immunol*. 2013;6(6):1110–1118.
15. Furuta GT, et al. Hypoxia-inducible factor 1-dependent induction of intestinal trefoil factor protects barrier function during hypoxia. *J Exp Med*. 2001;193(9):1027–1034.
16. Louis NA, Hamilton KE, Canny G, Shekels LL, Ho SB, Colgan SP. Selective induction of mucin-3 by hypoxia in intestinal epithelia. *J Cell Biochem*. 2006;99(6):1616–1627.
17. Masterson JC, et al. Local hypersensitivity reaction in transgenic mice with squamous epithelial IL-5 overexpression provides a novel model of eosinophilic oesophagitis. *Gut*. 2014;63(1):43–53.
18. Bruning U, et al. MicroRNA-155 promotes resolution of hypoxia-inducible factor 1α activity during prolonged hypoxia. *Mol Cell Biol*. 2011;31(19):4087–4096.
19. Weir L, Robertson D, Leigh IM, Vass JK, Pantelеyev AA. Hypoxia-mediated control of HIF/ARNT machinery in epidermal keratinocytes. *Biochim Biophys Acta*. 2011;1813(1):60–72.
20. Uchida T, et al. Prolonged hypoxia differentially regulates hypoxia-inducible factor (HIF)-1alpha and HIF-2α expression in lung epithelial cells: implication of natural antisense HIF-1α. *J Biol Chem*. 2004;279(15):14871–14878.
21. Lin Q, Cong X, Yun Z. Differential hypoxic regulation of hypoxia-inducible factors 1α and 2α. *Mol Cancer Res*. 2011;9(6):757–765.
22. Fang Y, Sullivan R, Graham CH. Confluence-dependent resistance to doxorubicin in human MDA-MB-231 breast carcinoma cells requires hypoxia-inducible factor-1 activity. *Exp Cell Res*. 2007;313(5):867–877.
23. Depping R, Jelkmann W, Kosyna FK. Nuclear-cytoplasmatic shuttling of proteins in control of cellular oxygen sensing. *J Mol Med*. 2015;93(6):599–608.
24. Singh LD, Singh SP, Handa RK, Ehmann S, Snyder AK. Effects of ethanol on GLUT1 protein and gene expression in rat astrocytes. *Metab Brain Dis*. 1996;11(4):343–357.
25. Griffin ME, et al. Post-transcriptional regulation of glucose transporter-1 by an AU-rich element in the 3′UTR and by hnRNP A2. *Biochem Biophys Res Commun*. 2004;318(4):977–982.
26. Campbell EL, et al. Transmigrating neutrophils shape the mucosal microenvironment through localized oxygen depletion to influence resolution of inflammation. *Immunity*. 2014;40(1):66–77.
27. Ebert BL, Firth JD, Ratcliffe PJ. Hypoxia and mitochondrial inhibitors regulate expression of glucose transporter-1 via distinct Cis-acting sequences. *J Biol Chem*. 1995;270(49):29083–29089.
28. Günzel D, Yu AS. Claudins and the modulation of tight junction permeability. *Physiol Rev*. 2013;93(2):525–569.
29. Furuse M, et al. Claudin-based tight junctions are crucial for the mammalian epidermal barrier: a lesson from claudin-1-deficient mice. *J Cell Biol*. 2002;156(6):1099–1111.
30. Björkman EV, Edebo A, Oltean M, Casselbrant A. Esophageal barrier function and tight junction expression in healthy subjects and patients with gastroesophageal reflux disease: functionality of esophageal mucosa exposed to bile salt and trypsin in vitro. *Scand J Gastroenterol*. 2013;48(10):1118–1126.
31. Abdulnour-Nakhoul SM, et al. Alterations in junctional proteins, inflammatory mediators and extracellular matrix molecules in eosinophilic esophagitis. *Clin Immunol*. 2013;148(2):265–278.
32. Katzka DA, et al. Effects of topical steroids on tight junction proteins and spongiosis in esophageal epithelia of patients with eosinophilic esophagitis. *Clin Gastroenterol Hepatol*. 2014;12(11):1824–1829.e1.
33. Lioni M, et al. Dysregulation of claudin-7 leads to loss of E-cadherin expression and the increased invasion of esophageal squamous cell carcinoma cells. *Am J Pathol*. 2007;170(2):709–721.
34. Boivin FJ, Schmidt-Ott KM. Transcriptional mechanisms coordinating tight junction assembly during epithelial differentiation. *Ann N Y Acad Sci*. 2017;1397(1):80–99.
35. Garcia-Hernandez V, Quiros M, Nusrat A. Intestinal epithelial claudins: expression and regulation in homeostasis and inflammation. *Ann N Y Acad Sci*. 2017;1397(1):66–79.
36. Nguyen N, et al. TGF-β1 alters esophageal epithelial barrier function by attenuation of claudin-7 in eosinophilic esophagitis. *Mucosal Immunol*. 2018;11(2):415–426.
37. Bedogni B, Welford SM, Cassarino DS, Nickoloff BJ, Giaccia AJ, Powell MB. The hypoxic microenvironment of the skin contributes to Akt-mediated melanocyte transformation. *Cancer Cell*. 2005;8(6):443–454.
38. Zhang X, et al. Impaired angiogenesis and mobilization of circulating angiogenic cells in HIF-1alpha heterozygous-null mice after burn wounding. *Wound Repair Regen*. 2010;18(2):193–201.
39. Zimmermann AS, et al. Epidermal or dermal specific knockout of PHD-2 enhances wound healing and minimizes ischemic injury. *PLoS One*. 2014;9(4):e93373.
40. Cowburn AS, Alexander LEC, Southwood M, Nizet V, Chilvers ER, Johnson RS. Epidermal deletion of HIF-2α stimulates wound closure. *J Invest Dermatol*. 2014;134(3):801–808.
41. Ma X, et al. Keloid-derived keratinocytes acquire a fibroblast-like appearance and an enhanced invasive capacity in a hypoxic microenvironment in vitro. *Int J Mol Med*. 2015;35(5):1246–1256.
42. Elson DA, Ryan HE, Snow JW, Johnson R, Arbeit JM. Coordinate up-regulation of hypoxia inducible factor (HIF)-1α and HIF-1 target genes during multi-stage epidermal carcinogenesis and wound healing. *Cancer Res*. 2000;60(21):6189–6195.
43. Zhang H, Nan W, Song X, Wang S, Si H, Li G. Knockdown of HIF-1α inhibits the proliferation and migration of outer root sheath cells exposed to hypoxia in vitro: an involvement of Shh pathway. *Life Sci*. 2017;191:82–89.
44. Huo X, et al. Hypoxia-inducible factor-2α plays a role in mediating oesophagitis in GORD. *Gut*. 2017;66(9):1542–1554.
45. Griffiths EA, et al. Increasing expression of hypoxia-inducible proteins in the Barrett's metaplasia-dysplasia-adenocarcinoma sequence. *Br J Cancer*. 2007;96(9):1377–1383.
46. Sallis BF, et al. A distinct esophageal mRNA pattern identifies eosinophilic esophagitis patients with food impactions. *Front Immunol*. 2018;9:2059.
47. Furuta GT, Katzka DA. Eosinophilic esophagitis. *N Engl J Med*. 2015;373(17):1640–1648.
48. Wang WS, Liang HY, Cai YJ, Yang H. DMOG ameliorates IFN-γ-induced intestinal barrier dysfunction by suppressing PHD2-dependent HIF-1α degradation. *J Interferon Cytokine Res*. 2014;34(1):60–69.
49. Liacouras CA, et al. Eosinophilic esophagitis: updated consensus recommendations for children and adults. *J Allergy Clin Immunol*. 2011;128(1):3–20.e6.
50. Lee JJ, et al. Hypoxia activates the cyclooxygenase-2-prostaglandin E synthase axis. *Carcinogenesis*. 2010;31(3):427–434.
51. Harada H, et al. Telomerase induces immortalization of human esophageal keratinocytes without p16INK4a inactivation. *Mol Cancer Res*. 2003;1(10):729–738.
52. Safran M, et al. Mouse model for noninvasive imaging of HIF prolyl hydroxylase activity: assessment of an oral agent that stimulates erythropoietin production. *Proc Natl Acad Sci U S A*. 2006;103(1):105–110.
53. McNamee EN, et al. Targeting granulocyte-macrophage colony-stimulating factor in epithelial and vascular remodeling in experimental eosinophilic esophagitis. *Allergy*. 2017;72(8):1232–1242.